





Ring of bound states in the continuum in the reciprocal space of a monolayer of high-contrast dielectric spheres

A. S. Kostyukov ¹, V. S. Gerasimov ^{1,2,*}, A. E. Ershov ^{1,2} and E. N. Bulgakov ³

¹*International Research Center of Spectroscopy and Quantum Chemistry, Siberian Federal University, 660041, Krasnoyarsk, Russia*

²*Institute of Computational Modelling SB RAS, 660036 Krasnoyarsk, Russia*

³*Kirensky Institute of Physics, Federal Research Center KSC SB RAS, 660036 Krasnoyarsk, Russia*



(Received 19 November 2021; revised 13 January 2022; accepted 14 January 2022; published 7 February 2022)

We consider light scattering by two-dimensional arrays of high-index dielectric spheres arranged into a triangular and square lattices. We demonstrate the appearance of the double degenerate accidental super-BIC modes with extremely suppressed radiative losses in the vicinity of the Γ point of the leaky band of the triangular lattice. Two rings of BICs (circular lines of BICs in reciprocal space) with different polarization appear at the point of the super-BIC destruction. The radius of the ring BIC (RBIC) changes as a function of the sphere's radius. We propose a generic analytical expression to describe the behavior of the guided mode decay rate as a function of the sphere radii and the wave vector in the vicinity of the RBIC. The results are explained using a multipolar approach.

DOI: [10.1103/PhysRevB.105.075404](https://doi.org/10.1103/PhysRevB.105.075404)

I. INTRODUCTION

All-dielectric nanophotonics is an extremely quickly developing area of modern optics. A great amount of scientific interest to the field was attracted due to the low losses and excellent resonant properties of high-index nanostructures [1–3]. All-dielectric nanophotonics is driven by the idea to utilize subwavelength dielectric nanoparticles with Mie resonances to create highly efficient optical metasurfaces and metadevices [4–6]. The most important examples of such dielectric structures are photonic crystal (PC) surfaces, which support electromagnetic (EM) modes with a high Q factor. Moreover, in the last decade, bound states immersed in the radiation continuum (BIC), formally with an infinite Q factor, have been actively studied. Such states in dielectric structures make it possible to localize light with extremely high intensity. BICs of different nature exist in infinite systems and are usually classified as symmetry protected, which cannot decay due to a different symmetry of radiation channels, and nontrivial (accidental), which arise with a special choice of structure parameters, due to destructive interference [7–11]. BICs of different nature have been discovered and investigated for the simplest optical systems—linear chain gratings, periodic arrays of rods, and PC surfaces.

Due to the translational symmetry of the system, the localization occurs only along one or two spatial directions. In a real experiment it is possible to fabricate finite systems (with finite number of unit cells N) of a small size with a high quality factor and a power-law behavior of $Q \sim N^\alpha$ employing the same BICs that exist in the infinite system [12–16]. This is one of the areas for engineering high- Q subwavelength dielectrics. By now BICs in all-dielectric structures are used

for other purposes as well. For example, the so-called Bloch BICs with a nonzero wave vector along the structure have a topological charge [9] and can be a source of polarization vortices in reciprocal space [17–19], which was experimentally observed in plane-wave scattering [20]. In addition, BICs with a topological charge can be successfully used for lasing [21,22].

Another interesting phenomena connected to the BICs is the emergence of exceptional points (EPs) [23]. Due to the accidental degeneracy of the dipole band with a BIC in the Γ point with the quadrupole band a linear Dirac cone in the dispersion relation is formed [24]. As the result of the further deformation of the cone due to the non-Hermitian perturbations, a circle of the EPs emerges in the reciprocal space. In addition, Bloch BICs collapsing with a small change in the parameters of the system can be formed in the vicinity of the Γ point [24].

Symmetry-protected BICs can be transformed into conventional high- Q resonances in a controlled manner when the inversion symmetry is broken [25–27]. This approach provides a design route to PC surfaces, enabling fine tuning of their spectral features.

All-dielectric structures supporting BICs can be a source of strong optical forces. For example, two PC slabs are capable of being attracted or repulsed by resonant optical forces that are much higher than the usual radiation pressure forces and grow proportionally to the Q factor [28]. Resonant optical forces lead to significant optomechanical effects [29] caused by elastic deformation. And, finally, let us note the promising prospects [30] in the use of PC surfaces in biosensorics due to the extreme sensitivity of BICs to small changes in the environment.

This work is devoted to special BIC transformations in a two-dimensional (2D) periodic system of high-contrast dielectric spheres—a monolayer (ML) of spheres. Despite its

*gerasimov@icm.krasn.ru

fabrication compatibility, such a system is less studied than PC slabs. The earliest numeric calculations of the optical response of MLs were performed by Ohtaka *et al.* [31–33] using the multipole expansion of the electromagnetic field (Mie theory). It was shown that a cluster of narrow Fano resonances in the reflectance is associated with interaction of a transmitted plane wave with long-lived bound states of the EM field.

Ohtaka *et al.* [33] indicates the existence of BICs in such a system at the Γ point of the leaky band (in modern terminology, symmetry-protected BICs). In [34], using the dipole approximation, the conditions under which reduced transmission or reflection of the incident wave is possible were studied. In [35], within the framework of the symmetry approach, the classification of the multipolar expansion of the EM field of ML was obtained, and the conditions for the existence of the BIC in the ML were derived.

Here we investigate special states that arise in the reciprocal space due to its topological nature, which we call the ring of BICs (RBICs), in a 2D periodic system of high-contrast dielectric spheres. For the first time such a class of resonant guided modes was discovered in PC slabs [16,36]. Specifically, these resonances arise when multiple BICs, each carrying a topological charge, merge in the reciprocal space and form a super-BIC [36] with radiation loss that follows the β_{\parallel}^6 law (here β_{\parallel} is the projection of the wave vector onto the ML plane). Radiation losses can be suppressed strongly in the vicinity of the Γ point. This turns out to be very useful for real dielectric systems consisting of a finite number of PC cells. The Q-factor of such a finite structure turns out to be much higher than in the case of finite structures supporting ordinary symmetry-protected BIC. In the end this leads to a dramatic drop of the lasing threshold [36].

In contrast to the case described in [16,36] where at the Γ point the symmetry-protected BIC always exist, in our case the RBICs with different polarizations appear with the destruction of the accidental BIC. The RBICs start to appear from the Γ point in the reciprocal space when the accidental BIC is destroyed due to the change in the radius of the spheres (or ML period with fixed sphere radius). The RBICs radius is extremely sensitive to changes of geometry parameters. In the vicinity of the RBICs, strong suppression of the mode's decay rate takes place, $\gamma \sim \beta_{\parallel}^4$. Moreover, we derive universal behavior of decay as a function of the wave vector and spheres radius.

II. METHOD

In two earlier papers [31,32] the well-known KKR (Korringa-Kohn-Rostoker) formalism designed to calculate the electronic band structure was applied to solve the problem of electromagnetic waves passing through a 2D periodic array of dielectric spheres. In a slightly different version, this method was described in [37]. The idea is that the electromagnetic field inside and outside the dielectric spheres is represented as a sum over vector spherical harmonics. In this approach it is possible to obtain a system of linear equations for the amplitudes of harmonics, while the matrix of the system is expressed in terms of a t matrix describing the Mie scattering of the individual sphere and the structural

factor Γ , which depend only on the type of lattice and the frequency of the field. Within the framework of this formalism [38] the band structure of a 2D lattice of spheres can be calculated taking into account the radiation decay. To do this it is necessary to find the poles of the dispersion equation for complex frequency values $k_0 = \omega/c$. The EM field calculated for the pole is a resonant mode with a Q factor equal to $Q = -\Re(k_0)/2\Im(k_0)$ with the decay rate of resonant modes $\gamma = -2\Im(k_0)$, which is equal to the FWHM on the transmission spectra.

In this paper the multipole approach in the [31,32] variant was used for numerical simulations of the scattering of plane waves by a 2D lattice of spheres, the band structure and decay of resonant modes, as well as for the theoretical interpretation of the obtained results.

We also used the MULTEM Mie software to calculate the transmission spectrum of the structure. The advantage of MULTEM is the ability to calculate the transmission coefficient for the infinite periodic array of NPs in the frequency domain in a tiny portion of a second. It allows analysis of a large amount of spectral data and can directly determine the spectral position and the Q factor of the resonance [39].

III. RESULTS

A. Accidental BIC at Γ point of ML

The structures under consideration are infinite 2D arrays or monolayers of spherical NPs of radius R with a distance between the centers of the nearest particles a . Hereafter we use dimensionless R and k : $R = R'/a$ and $k = k' \cdot a$, where R' , a are NP radius and structure period in meters and k' is wave vector in meters⁻¹. Triangular and square lattices are considered [see Figs. 1(a) and 1(b)].

The modes that are supported by the ML can be divided into three categories:

- (i) pure modes with infinite lifetimes that are located below the light line;
- (ii) delocalized resonant modes with a finite lifetime located above the light line; and
- (iii) two types of localized modes above the line of light: symmetry protected and accidental.

When plane waves are scattered by the ML, these usually long-lived resonant modes manifest themselves as Fano resonances in the transmission spectrum. At the resonance point, the mode is strongly excited, which leads to a sharp increase in amplitude of EM field in the vicinity of the ML. The BIC in the scattering pattern appear as a collapse of the Fano resonance with a variation of the parameters, i.e., the direction of the wave vector or a physical parameter of the system, in our case the radius of the spheres. The collapse of the Fano resonance is frequently used to observe BIC in the system. In Figs. 1(c) and 1(d) we show the transmission spectra at normal incidence. In this case the symmetry-protected BICs do not appear in the spectra. However, the presence of accidental BICs at the Γ point is clearly seen in the points marked as 1,2,3. Their exact positions and the twofold-degenerate mode profiles are shown in Figs. 1(c), 1(d) and 1(e). Two degenerate BICs in the Γ point for a certain $R = R_c$ (here R_c is

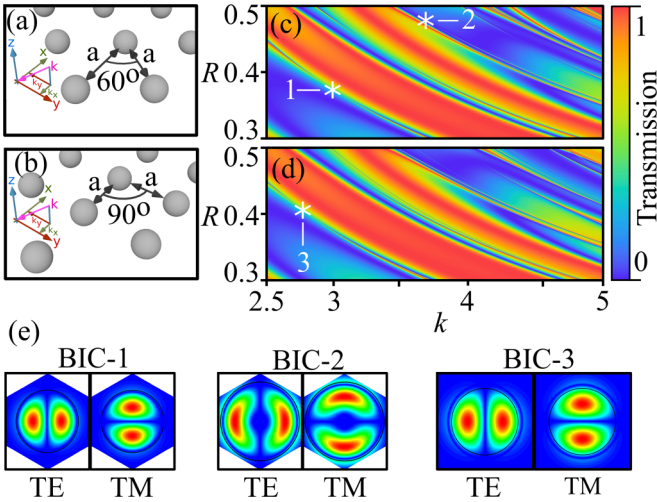


FIG. 1. The sketch of 2D array of dielectric NPs with $\varepsilon = 15$ in a homogeneous environment with $\varepsilon = 1$, (a) triangular packing and (b) square packing, (c, d) transmission spectra for corresponding arrays and various radius of the sphere and wave vector at the Γ point, showing three bound states in the continuum considered in the paper: BIC-1 with $R_c = 0.3764$, $k_0 = 2.985$; BIC-2 with $R_c = 0.4778$, $k_0 = 3.669$; BIC-3 with $R_c = 0.4049$, $k_0 = 2.771$. (e) Corresponding wave functions (H_z component of the EM field). R_c is the critical radius of spheres with accidental BIC at the Γ point.

the critical radius of NPs) which is transverse electric/transverse magnetic (TE/TM)-like belong to two different leaky bands. In the vicinity of the Γ point in these bands, the states with abnormally low decay rate appear with a slight change in R , as can be seen in Fig. 2.

B. Ring of BICs

The doubly degenerate accidental BIC in the center of the band is not stable and disappears if the ML parameters change. In the case of a triangular lattice, this destruction occurs with the simultaneous emergence of 12 accidental BICs in the reciprocal space with wave vectors directed strictly along the ML symmetry axes and which are located precisely on the ring $k_x^2 + k_y^2 = k_r^2$ of resonant modes with an extremely large Q -factor ($Q > 10^{11}$) (RBIC). One RBIC with TM-like polarization emerge if $R > R_c$, and another

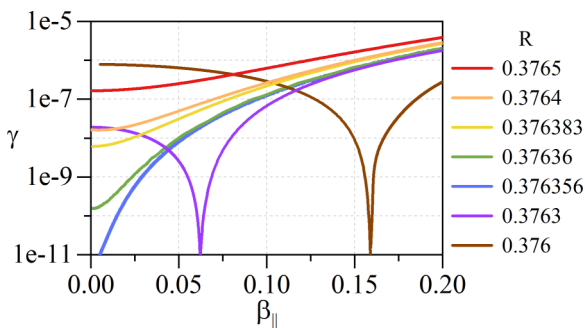


FIG. 2. The decay rate of resonant modes γ for BIC-1 (see Fig. 1) and TE polarization as a function of β_{\parallel} for various particle sizes R .

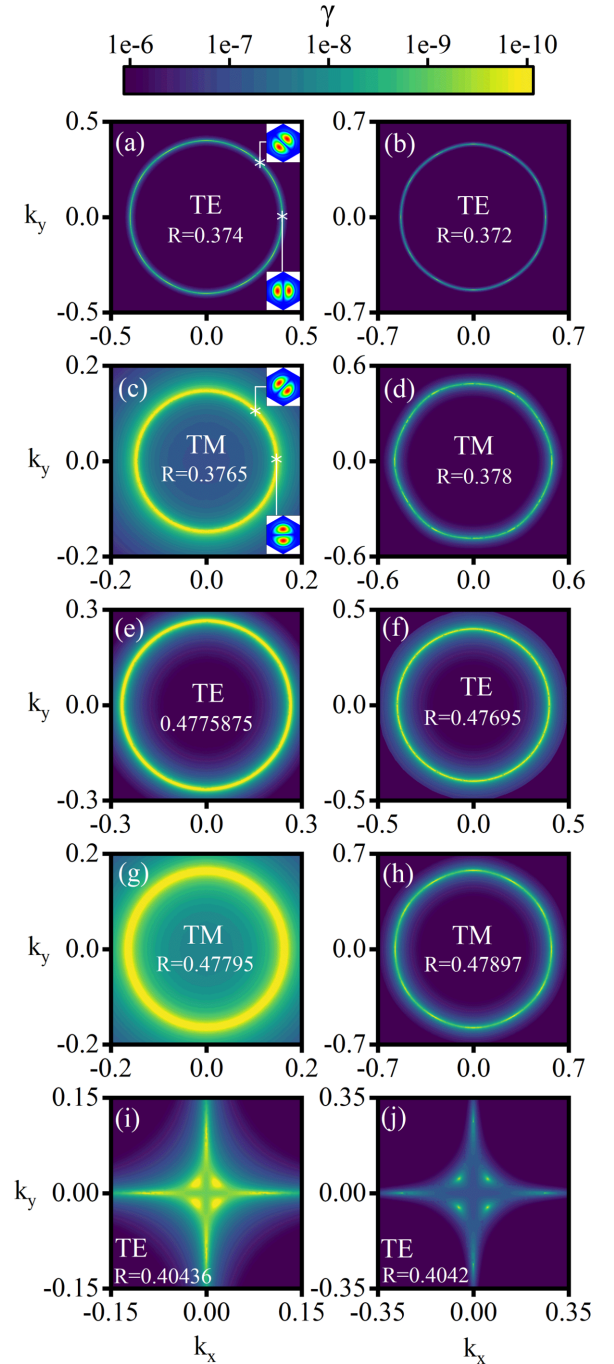


FIG. 3. γ for BIC bands for triangular lattice in dependence of k_x , k_y for different R . For BIC-1: (a, b) TE polarization, $R < R_c$; (c, d) TM polarization, $R > R_c$. For BIC-2: (e, f) TE polarization, $R < R_c$; (g, h) TM polarization, $R > R_c$. For BIC-3: (i, j) TE polarization for square lattice, $R < R_c$. The insets at (a, c) H_z component of wave functions corresponding to the marked positions at RBICs.

one with TE-like polarization if $R < R_c$ [see Figs. 3(a)–3(h)]. To be precise, the concept of polarization of resonant modes cannot be formally defined for a photonic crystal (PhC) slab [40]. In our case, by polarization we will understand the ability to interact (to be excited) by a plane wave with corresponding polarization. Figure 3 clearly demonstrates the emergence of RBIC of TE and TM polarization in

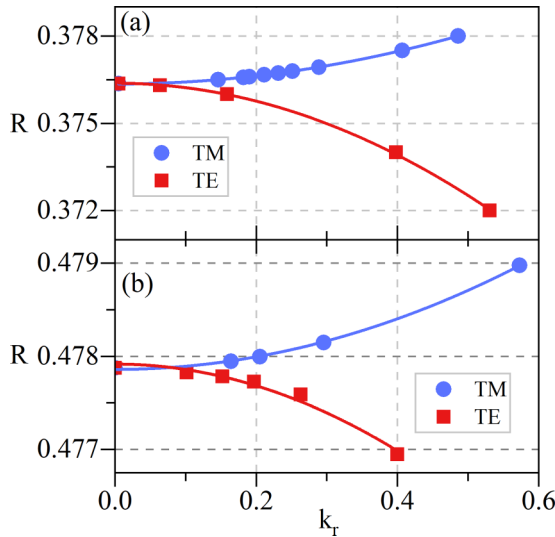


FIG. 4. RBIC radius k_r and corresponding particle size R for TE and TM polarization. (a) BIC-1 and (b) BIC-2. Approximations $R(k_r) = C + D \cdot k_r^2$ were performed with coefficients $C_{\text{BIC-1}}^{\text{TE}} = 0.37638$, $D_{\text{BIC-1}}^{\text{TE}} = -0.01541$, $C_{\text{BIC-1}}^{\text{TM}} = 0.37635$, $D_{\text{BIC-1}}^{\text{TM}} = 0.00697$, $C_{\text{BIC-2}}^{\text{TE}} = 0.47792$, $D_{\text{BIC-2}}^{\text{TE}} = -0.00581$, $C_{\text{BIC-2}}^{\text{TM}} = 0.47786$, $D_{\text{BIC-2}}^{\text{TM}} = 0.00339$.

reciprocal space in the case of the triangular lattices, as well as the fact that in the case of the square lattice RBIC is not formed. In Figs. 3(a) and 3(c) we show the field profiles of resonant modes with different polarizations located on the RBIC for the $\varphi = \pi/4$ angle ($k_x = k_r \cos \varphi$, $k_y = k_r \sin \varphi$). For small RBIC radii k_r , the wave functions look almost the same as in the case of the BIC in the band center [see Fig. 1(e)]; however, the wave functions are rotated by an angle φ .

A remarkable fact is that the RBICs radius k_r strongly depends on the radius of the spheres. It can be clearly seen in Fig. 4. Even a tiny change of one ten thousandth leads to a significant change in the position of RBICs.

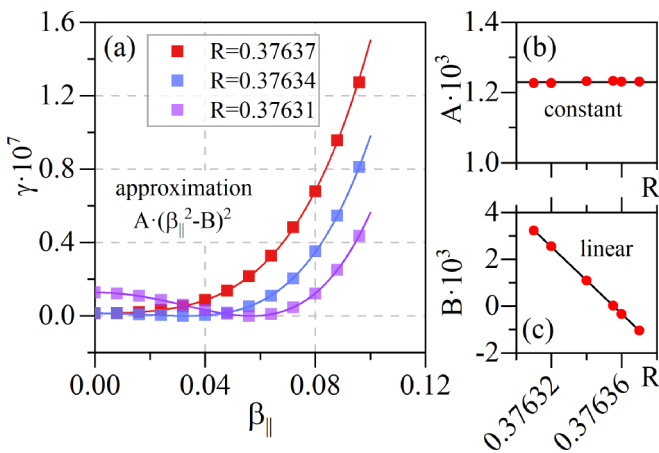


FIG. 5. (a) γ as a function of β_{\parallel} for various R of BIC-1 TE polarization. (b, c) Coefficients of $A \cdot (\beta_{\parallel}^2 - B)^2$ approximation depending on R .

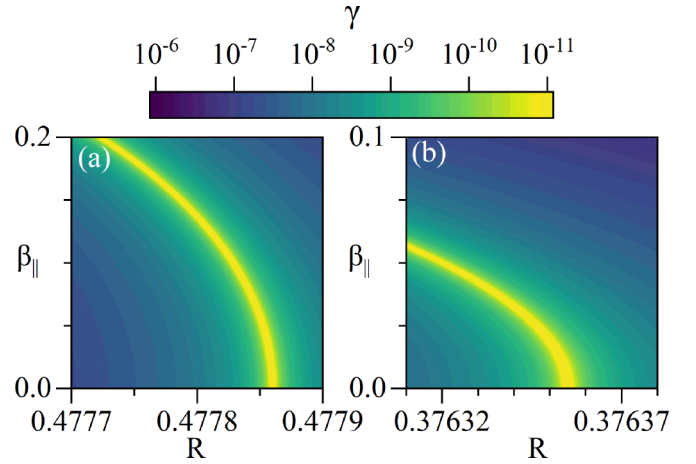


FIG. 6. γ for (a) BIC-1 and (b) BIC-2 (Fig. 1) and TE polarization with various β_{\parallel} .

In Fig. 5 we show the dependence of the decay rate of resonant modes γ as the function of R and wave vector $\beta_{\parallel} = |\vec{\beta}_{\parallel}|$, $\vec{\beta}_{\parallel} = \vec{e}_x k_x + \vec{e}_y k_y$. In our case, γ differs greatly from the standard behavior $\gamma \sim \beta_{\parallel}^2$ and is analyzed in detail in the Appendix. Here we consider $\vec{\beta}_{\parallel}$ is directed along the symmetry axes. The decay rate γ follows the $\gamma = A(\beta_{\parallel}^2 - B)^2$ law precisely, wherein A is a constant depending only on polarization, and the parameter B , which is the key parameter to determine $k_r = \sqrt{B}$, depends on both polarization and $\Delta R = R - R_c$. As follows from Fig. 5, the dependence of B on R is linear; therefore, at the RBIC collapse point the decay law transforms into a power function, $\gamma = A\beta_{\parallel}^4$.

An intriguing feature of the square lattice is that there are no RBICs formed in the vicinity of BIC-3 with the change of the spheres radius R . Nevertheless, eight accidental BICs with $\beta_{\parallel} \neq 0$ emerge in the center of the band along the symmetry axes when the accidental BIC is destroyed at the Γ point [see Figs. 3(i) and 3(j)]. The newly formed accidental BICs drift away with different velocities from the Γ point when R is changed so that no RBICs can be formed. For each direction mentioned, there is still a common decay rate behavior $\gamma = A(\beta_{\parallel}^2 - B)^2$ but with different values of parameters A and B .

Using the obtained dependencies, we present the behavior of the BIC (for BIC-1 and BIC-2) near the corresponding resonance points as approximations by a function $\gamma(R, \beta_{\parallel}) = A \cdot [\beta_{\parallel}^2 - B(R)]^2$ with a linear dependence $B(R)$. The resulting plots are shown in Figs. 6(a) and 6(b), respectively.

These calculations were performed for TE polarized light. The behavior of the RBIC will differ for TM polarization in that the ring appears at $R > R_c$ as demonstrated in Fig. 4. The TE and TM polarizations are obviously identical at normal incidence, so the curves describing the position (radius) of the ring for the different polarizations converge at $\beta_{\parallel} = 0$ to a point $R = R_c$.

C. Conclusion

Super BIC is a BIC with extremely suppressed losses in the vicinity of the Γ point. This concept was first proposed in Refs. [16,36] for PhC slabs and are associated with merging of

multiple accidental BICs. As usual, a whole line of extremely high- Q resonances is formed in its vicinity. In this paper we continue to study this new class of high- Q modes for the case of a 2D triangular lattice of dielectric spheres which was called a ring of BICs in the reciprocal space. The origin of RBICs is different from that discussed in [16,36]. Two RBICs of different polarizations appear with the destruction of twofold-degenerate accidental super-BIC as a function of the radius of the spheres (or lattice constant). True BICs (Q is infinite) which belong to the RBICs are located on the symmetry axes of the lattice. In the vicinity of the RBICs there is a significant suppression of the loss of guided modes and a universal behavior of damping rate as a function of the radius of the sphere and the wave vector, which can be explained in terms of multipolar theory.

The possibility of the existence of a line of BICs for meta-atoms packed in a subwavelength lattice was hypothetically discussed using a multipolar approach. However, its origin was not associated with super-BIC but only with the presence of a large-amplitude octupole in modal expansion which has a nodal cone. RBICs were also observed for the triangular lattice of spheres near a Dirac cone [24], and its existence was ensured due to the interaction of two photonic bands with strong and weak damping. As it turned out, the anomalous suppression of decay rate caused by super-BIC leads to a significant increase in Q factor of the finite system and can be used in optoelectronic devices, for example, to reduce the lasing threshold power.

Moreover, a particularly interesting feature of RBIC is the fact that the polarization of the BIC continuously changes along the ring, making a full turn. We expect that this fact can be used to generate optical vortices as shown in [19].

ACKNOWLEDGMENTS

This research was supported by RFBR, Krasnoyarsk Territory, and Krasnoyarsk Regional Fund of Science, Project No. 20-42-240003, by the Ministry of Science and Higher Education of the Russian Federation, Project No. FSRZ-2020-0008.

APPENDIX

The theory which allows one to calculate the decay rate of quasi-BIC under the conditions of weak symmetry break is developed in [27]. The decay rate has a universal behavior as a function of the symmetry-breaking parameter. The decay rate is expressed via overlap coefficients between the mode profile inside the PC and the vertically propagating plane wave. In this section we will show that similar expressions can also be obtained using modal decomposition over spherical vector harmonics.

The scattering wave function outside the ML in the KKR method is expressed in terms of vector spherical harmonics:

$$\begin{aligned} \vec{E}_{sc}(\vec{r}) = & \sum_{\vec{R}_j \in \Lambda} \sum_{nm} [a_{nm} e^{i\vec{\beta}_{||} \cdot \vec{R}_j} \vec{M}_{nm}^{(3)}(k_0, \vec{r}_j) \\ & + b_{nm} e^{i\vec{\beta}_{||} \cdot \vec{R}_j} \vec{N}_{nm}^{(3)}(k_0, \vec{r}_j)], \end{aligned} \quad (\text{A1})$$

where $\vec{r}_j = \vec{r} - \vec{R}_j$, $\sum_{nm} \equiv \sum_{n=1}^{\infty} \sum_{m=-n}^n$, while \vec{R}_j iterates over the Bravais lattice (Λ). We assume that the system is excited by an external plane wave with a wave vector along the ML plane. It is also assumed that the amplitudes of vector spherical harmonics a_{nm} , b_{nm} are known as a result of numerical calculation using the KKR method. In a far field the scattered field in Eq. (A1) should be a superposition of plane waves. In order to find this decomposition, we apply the well-known summation equation to Eq. (A1) [41],

$$\begin{aligned} \vec{E}_{sc}(\vec{r}) = & \sum_{\vec{p}_g \in \Lambda^*} \left(\frac{2\pi i^{-n}}{k_0 k_{g,z}^+ A_2} \right) \left[\sum_{nm} [a_{nm} \vec{X}_{nm}(\hat{k}_g^{\pm}) + ib_{nm} \vec{Z}_{nm}(\hat{k}_g^{\pm})] \right] \\ & \times e^{i\vec{k}_g^{\pm} \cdot \vec{r}} \begin{cases} + & \text{for } z > 0 \\ - & \text{for } z < 0, \end{cases} \end{aligned} \quad (\text{A2})$$

where \vec{p}_g iterates over the reciprocal lattice (Λ^*), $\vec{k}_g^{\pm} = \vec{\beta}_{||} + \vec{p}_g \pm \vec{e}_z \sqrt{k_0^2 - (\vec{\beta}_{||} + \vec{p}_g)^2}$, $k_{g,z}^{\pm} = \sqrt{k_0^2 - (\vec{\beta}_{||} + \vec{p}_g)^2}$, and A_2 is the unit cell area $A_2 = |\vec{a} \times \vec{b}|$, where \vec{a} , \vec{b} are the basis vectors of the Bravais lattice, and the symbol $\hat{\cdot}$ denotes the unit vector. Additionally,

$$\begin{aligned} \vec{M}_{nm}^{(3)}(k_0, \vec{r}) = & h_n(k_0 r) \vec{X}_{nm}(\Theta, \varphi) \\ \vec{Z}_{nm} = & [\vec{e}_r \times \vec{X}_{nm}], \end{aligned} \quad (\text{A3})$$

where X and Z are the angular parts of the spherical vector harmonics.

Suppose that only one diffraction channel is open, i.e., $k_0^2 > (\vec{\beta}_{||} + \vec{p}_g)^2$ only for $\vec{p}_g = 0$. In this case, in the upper half space ($z > 0$) we have a single plane wave in the far field which reads as

$$\vec{E}_{sc}(\vec{r}) = C \sum_{nm} i^{-n} [a_{nm} \vec{X}_{nm}(\hat{k}_0) + ib_{nm} \vec{Z}_{nm}(\hat{k}_0)] e^{i\vec{k}_0 \cdot \vec{r}}. \quad (\text{A4})$$

Here $\vec{k}_0 = \vec{\beta}_{||} + \vec{e}_z \sqrt{k_0^2 - \beta_{||}^2}$, $C = 2\pi / (k_0 k_z A_2)$. The scattering wave function [Eq. (A4)] appears when a plane wave with a wave vector \vec{k}_0 is scattered. Let $\vec{\beta}_{||}$ be directed along one of the lattice symmetry axes, X . When mirrored relative to the (XOZ) plane, the field components take the following form [42]:

$$\begin{aligned} E_x(x, -y, z), -E_y(x, -y, z), E_z(x, -y, z) \\ H_x(x, -y, z), -H_y(x, -y, z), H_z(x, -y, z). \end{aligned} \quad (\text{A5})$$

The fields in Eq. (A5) are also a solutions of Maxwell's equations. There are even and odd solutions:

$$\hat{\Lambda} \vec{E}(\vec{r}) = (-1)^S \vec{E}(\vec{r}), \quad S = \begin{cases} 0, & \text{even} \\ 1, & \text{odd} \end{cases}. \quad (\text{A6})$$

Even solutions are obtained when the system is excited by a TM; plane-wave, odd solutions are obtained when excited by an TE wave. It is easy to check that in this case

$$\begin{aligned} a_{nm} = & (-1)^{S+m+1} a_{n,-m} \\ b_{nm} = & (-1)^{S+m} b_{n,-m} \end{aligned}$$

Accordingly, the components of a plane wave in the single-channel case are equal to

$$\begin{aligned}
E_\theta &= C \sum_{n,m \geq 0} i^{-n} [1 + (-1)^S (1 - \delta_{m0})] \cdot \frac{(-1)^m}{\sqrt{n(n+1)}} \left[a_{nm} \left(\frac{im}{\sin \theta_{k_0}} \right) P_n^m(\cos \theta_{k_0}) + ib_{nm} \left(\frac{\partial}{\partial \theta_{k_0}} P_n^m(\cos \theta_{k_0}) \right) \right], \\
E_\phi &= C \sum_{n,m \geq 0} i^{-n} [1 + (-1)^{S+1} (1 + \delta_{m0})] \cdot \frac{(-1)^m}{\sqrt{n(n+1)}} \left[-a_{nm} \left(\frac{\partial P_n^m(\cos \theta_{k_0})}{\partial \theta_{k_0}} \right) + ib_{nm} \frac{im}{\sin \theta_{k_0}} P_n^m(\cos \theta_{k_0}) \right]. \quad (\text{A7})
\end{aligned}$$

Here $P_n^m(x)$ are normalized associated Legendre functions. Let us also introduce the following functions:

$$\pi_n^m(\theta) = \frac{1}{\sin \theta} P_n^m(\cos \theta); \quad \tau_n^m = \frac{d}{d\theta} P_n^m(\cos \theta). \quad (\text{A8})$$

Here we consider the limiting case $\theta \rightarrow 0$. Then [43]

$$\begin{aligned}
P_n^m(\cos \theta) &\approx C_{nm} \frac{(m+n)!}{(n-m)!} \left(\frac{2}{2n+1} \right)^m J_m \left(\frac{2n+1}{2} \theta \right) \\
\pi_n^m(\theta) &\approx C_{nm} \frac{1}{2} \frac{(n+m)!}{(n-m)!(m-1)!} \left(\frac{\theta}{2} \right)^{m-1} \\
\tau_n^m &\approx \pi_n^m(\theta), \quad C_{nm} = \sqrt{\frac{2n+1}{2} \frac{(n-m)!}{(n+m)!}}. \quad (\text{A9})
\end{aligned}$$

Precisely in the Γ point ($\theta_{k_0} = 0$) the contributions to Eq. (A7) with $m = 0, 2, 3, \dots$ automatically nullify. A nonzero contribution is provided by a sum term with $m = 1$ [35].

Bound states in a continuum are a special class of solutions of Maxwell's equations that exist without a source and are nonradiative due to the conservation of energy. In the Γ point it becomes possible only if $a_{n,m=1} = b_{n,m=1} = 0$. Such BICs are called symmetry protected [9]. One more BIC type are accidental or non-symmetry-protected BICs. In this case,

$$\begin{aligned}
E_\theta &= -C[1 + (-1)^S] i \sum_{n=1}^{\infty} i^{-n} \frac{a_{n,1} + b_{n,1}}{\sqrt{n(n+1)}} \pi_n^1(0) = 0, \\
E_\phi &= -C[1 + (-1)^{S+1}] \sum_{n=1}^{\infty} i^{-n} \frac{a_{n,1} + b_{n,1}}{\sqrt{n(n+1)}} \pi_n^1(0) = 0. \quad (\text{A10})
\end{aligned}$$

Here $\pi_n^1(0) = \tau_n^1(0) = 1/4\sqrt{2n(n+1)(2n+1)}$. Thus the accidental BIC is possible if for some $k_0 = k_{0B}$,

$$\sum_{n=1}^{\infty} \frac{i^{-n}}{\sqrt{n(n+1)}} (a_{n,1} + b_{n,1}) \pi_n^1(0) = 0. \quad (\text{A11})$$

All the terms in Eq. (A11) $i^{-n} a_{n,1}$, $i^{-n} b_{n,1}$ are real up to the common phase [35]. k_{0B} is not an independent variable but is determined from the solution of Maxwell's equations under radiation boundary conditions. Nevertheless, by varying any parameter, for example, the radius of spheres, it is possible to achieve $\Im(k_{0B}) = 0$, or the validity of Eq. (A11).

It is possible to find the law of waveguide modes decay in the vicinity of the Γ point using the standard definition of the Q factor:

$$Q = \omega \frac{U}{P}, \quad (\text{A12})$$

where U is the mode energy and P is the radiation power. In our case of an infinite system, it is necessary to consider the

surface energy density as U in Eq. (A12) and the radiation intensity of a plane wave as P so that $P = c/(8\pi |\vec{E}_{sc}|^2)$. As far as $\omega a/c = k_0 a \sim 1$, in the case $Q \gg 1$ we obtain the estimation $U \gg |\vec{E}_{sc}|^2 a$. The resonant mode is determined up to a constant multiplier, so we fixate the amplitudes a_{nm} , b_{nm} by the condition $\sum_{nm} (|a_{nm}|^2 + |b_{nm}|^2) = 1$.

In the vicinity of super-BIC (R_b point), with a small change of $R = R_b + \Delta R$, the value $|\vec{E}_{sc}|^2$ crosses zero, while U is just slightly changed due to the small change of a_{nm} and b_{nm} . Therefore in the vicinity of super-BIC we have the following estimation for the Q factor:

$$Q \approx \frac{\lambda}{|\vec{E}_{sc}|^2}, \quad -\Im(k_0) \approx \left(\frac{k_{0B}}{2} \right) \frac{|\vec{E}_{sc}|^2}{\lambda}, \quad (\text{A13})$$

where λ is some constant. In Fig. 7 we show the comparison of $-\Im(k_0)$ calculated using Eq. (A13) with an exact procedure for numerical search for the poles. As one can see, Eq. (A13) provides good accuracy. Since the expansion for amplitudes in Eq. (A10) begins with linear terms,

$$\begin{aligned}
a_{n,1}^{(S)}(R) &\approx a_{n,1}^{(S)}(R_b) + A_n^{(S)} \Delta R, \\
b_{n,1}^{(S)}(R) &\approx b_{n,1}^{(S)}(R_b) + B_n^{(S)} \Delta R, \quad (\text{A14})
\end{aligned}$$

therefore, using Eqs. (A10) and (A13) we can conclude that $-\Im(k_0^{(S)}) \sim \Delta R^2$, which is also confirmed by Fig. 7.

Let us write the Eq. (A10) for $\theta_{k_0} \neq 0$ ($\theta_{k_0} = \frac{\beta_{||}}{k_0}$) to evaluate the behavior of the pole at $\beta_{||} \rightarrow 0$:

$$\begin{aligned}
E_\theta^{(S)} &= -C[1 + (-1)^S] \sum_{n=1}^{\infty} \frac{i^{-n}}{\sqrt{n(n+1)}} \\
&\times [a_{n,1}^{(S)}(R, \theta_{k_0}) \pi_{n,1}(\theta_{k_0}) + b_{n,1}^{(S)}(R, \theta_{k_0}) \tau_{n,1}(\theta_{k_0})],
\end{aligned}$$

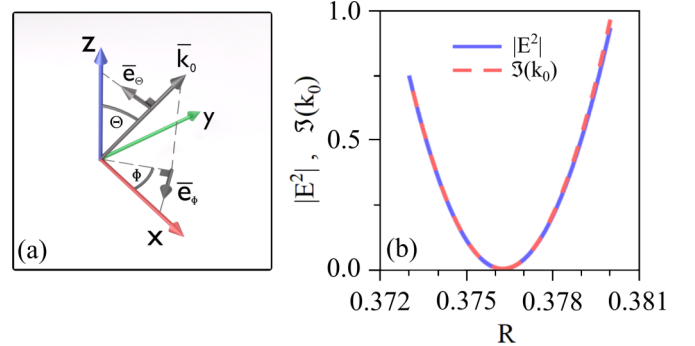


FIG. 7. (a) Definition of the vectors and angles of the system. (b) Normalized $|E^2|$ and $\Im(k_0)$ dependencies of R in the vicinity of accidental BIC for BIC-1.

$$E_{\phi}^{(S)} = C[1 + (-1)^{S+1}] \sum_{n=1}^{\infty} \frac{i^{-n}}{\sqrt{n(n+1)}} \times [a_{n,1}^{(S)}(R, \theta_{k_0})\pi_{n,1}(\theta_{k_0}) + b_{n,1}^{(S)}(R, \theta_{k_0})\tau_{n,1}(\theta_{k_0})]. \quad (\text{A15})$$

Due to the symmetry the decomposition of $a_{n,1}^{(S)}, b_{n,1}^{(S)}$ by θ starts with quadratic terms:

$$\begin{aligned} a_{n,1}^{(S)}(R, \theta) &\approx a_{n,1}^{(S)}(R_b, 0) + A_n^{(S)}\Delta R + \gamma_n^{(S)}\theta^2, \\ b_{n,1}^{(S)}(R, \theta) &\approx b_{n,1}^{(S)}(R_b, 0) + B_n^{(S)}\Delta R + \delta_n^{(S)}\theta^2. \end{aligned} \quad (\text{A16})$$

Besides,

$$\begin{aligned} \pi_{n,1}(\theta) &\approx \pi_{n,1}(0) + \alpha_n\theta^2, \\ \tau_{n,1}(\theta) &\approx \tau_{n,1}(0) + \beta_n\theta^2. \end{aligned} \quad (\text{A17})$$

After substituting Eq. (A16) and Eq. (A17) into Eq. (A15), we find

$$|\vec{E}_{sc}^{(S)}|^2 = |A^{(S)}\Delta R + B^{(S)}\theta_{k_0}^2|^2 \quad (\text{A18})$$

or

$$\Im(k_0) = C_S |\Delta R + \lambda^{(S)}k_x^2|^2. \quad (\text{A19})$$

One can make sure that for $\theta_{k_0} \neq 0$, the contributions with $m \neq 1$ in Eq. (A7) become nonzero and provide the correction to the amplitudes of $\sim \theta^2$ for square and $\sim \theta^4$ for triangular lattices, so that the result in Eqs. (A18) and (A19) does not change in the leading order. Moreover, $\lambda^{(S)}$ in Eq. (A19) is real; therefore there is always a solution, $\Im(\omega) = 0$, for $k_x = \sqrt{|\Delta R/\lambda^{(S)}|}$.

-
- [1] P. Tonkaev and Y. Kivshar, High-q dielectric Mie-resonant nanostructures (brief review), *JETP Lett.* **112**, 615 (2020).
- [2] S. Kruk and Y. Kivshar, Functional meta-optics and nanophotonics governed by Mie resonances, *ACS Photonics* **4**, 2638 (2017).
- [3] K. Koshelev, G. Favraud, A. Bogdanov, Y. Kivshar, and A. Fratalocchi, Nonradiating photonics with resonant dielectric nanostructures, *Nanophotonics* **8**, 725 (2019).
- [4] S. Fan and J. D. Joannopoulos, Analysis of guided resonances in photonic crystal slabs, *Phys. Rev. B* **65**, 235112 (2002).
- [5] A. E. Miroshnichenko, S. Flach, and Y. S. Kivshar, Fano resonances in nanoscale structures, *Rev. Mod. Phys.* **82**, 2257 (2010).
- [6] V. Astratov, J. Culshaw, R. Stevenson, D. Whittaker, M. Skolnick, T. Krauss, and R. de la Rue, Resonant coupling of near-infrared radiation to photonic band structure waveguides, *J. Lightwave Technol.* **17**, 2050 (1999).
- [7] V. Pacradouni, W. J. Mandeville, A. R. Cowan, P. Paddon, J. F. Young, and S. R. Johnson, Photonic band structure of dielectric membranes periodically textured in two dimensions, *Phys. Rev. B* **62**, 4204 (2000).
- [8] P. Paddon and J. F. Young, Two-dimensional vector-coupled-mode theory for textured planar waveguides, *Phys. Rev. B* **61**, 2090 (2000).
- [9] C. W. Hsu, B. Zhen, A. D. Stone, J. D. Joannopoulos, and M. Soljačić, Bound states in the continuum, *Nat. Rev. Mater.* **1**, 16048 (2016).
- [10] E. N. Bulgakov and A. F. Sadreev, Light trapping above the light cone in a one-dimensional array of dielectric spheres, *Phys. Rev. A* **92**, 023816 (2015).
- [11] X. Gao, C. W. Hsu, B. Zhen, X. Lin, J. D. Joannopoulos, M. Soljačić, and H. Chen, Formation mechanism of guided resonances and bound states in the continuum in photonic crystal slabs, *Sci. Rep.* **6**, 31908 (2016).
- [12] E. N. Bulgakov and A. F. Sadreev, High-q resonant modes in a finite array of dielectric particles, *Phys. Rev. A* **99**, 033851 (2019).
- [13] Z. F. Sadrieva, M. A. Belyakov, M. A. Balezin, P. V. Kapitanova, E. A. Nenasheva, A. F. Sadreev, and A. A. Bogdanov, Experimental observation of a symmetry-protected bound state in the continuum in a chain of dielectric disks, *Phys. Rev. A* **99**, 053804 (2019).
- [14] E. N. Bulgakov and D. N. Maksimov, q -factor optimization in dielectric oligomers, *Phys. Rev. A* **100**, 033830 (2019).
- [15] D. F. Kornovan, R. S. Savelev, Y. S. Kivshar, and M. I. Petrov, High-q localized states in finite arrays of subwavelength resonators, *ACS Photonics* **8**, 3627 (2021).
- [16] M.-S. Hwang, H.-C. Lee, K.-H. Kim, K.-Y. Jeong, S.-H. Kwon, K. Koshelev, Y. Kivshar, and H.-G. Park, Ultralow-threshold laser using super-bound states in the continuum, *Nat. Commun.* **12**, 4135 (2021).
- [17] E. N. Bulgakov and D. N. Maksimov, Bound states in the continuum and polarization singularities in periodic arrays of dielectric rods, *Phys. Rev. A* **96**, 063833 (2017).
- [18] W. Liu, B. Wang, Y. Zhang, J. Wang, M. Zhao, F. Guan, X. Liu, L. Shi, and J. Zi, Circularly Polarized States Spawning from Bound States in the Continuum, *Phys. Rev. Lett.* **123**, 116104 (2019).
- [19] B. Wang, W. Liu, M. Zhao, J. Wang, Y. Zhang, A. Chen, F. Guan, X. Liu, L. Shi, and J. Zi, Generating optical vortex beams by momentum-space polarization vortices centred at bound states in the continuum, *Nat. Photonics* **14**, 623 (2020).
- [20] Y. Zhang, A. Chen, W. Liu, C. W. Hsu, B. Wang, F. Guan, X. Liu, L. Shi, L. Lu, and J. Zi, Observation of Polarization Vortices in Momentum Space, *Phys. Rev. Lett.* **120**, 186103 (2018).
- [21] C. Peng, Y. Liang, K. Sakai, S. Iwahashi, and S. Noda, Three-dimensional coupled-wave theory analysis of a centered-rectangular lattice photonic crystal laser with a transverse-electric-like mode, *Phys. Rev. B* **86**, 035108 (2012).
- [22] A. Kodigala, T. Lepetit, Q. Gu, B. Bahari, Y. Fainman, and B. Kanté, Lasing action from photonic bound states in continuum, *Nature (London)* **541**, 196 (2017).
- [23] B. Zhen, C. W. Hsu, Y. Igarashi, L. Lu, I. Kaminer, A. Pick, S.-L. Chua, J. D. Joannopoulos, and M. Soljačić, Spawning rings of exceptional points out of Dirac cones, *Nature (London)* **525**, 354 (2015).
- [24] E. N. Bulgakov and D. N. Maksimov, Bound states in the continuum and Fano resonances in the Dirac cone spectrum, *J. Opt. Soc. Am. B* **36**, 2221 (2019).

- [25] K. Koshelev, A. Bogdanov, and Y. Kivshar, Meta-optics and bound states in the continuum, *Sci. Bull.* **64**, 836 (2019).
- [26] A. C. Overvig, S. C. Malek, M. J. Carter, S. Shrestha, and N. Yu, Selection rules for quasibound states in the continuum, *Phys. Rev. B* **102**, 035434 (2020).
- [27] K. Koshelev, S. Lepeshov, M. Liu, A. Bogdanov, and Y. Kivshar, Asymmetric Metasurfaces with High- q Resonances Governed by Bound States in the Continuum, *Phys. Rev. Lett.* **121**, 193903 (2018).
- [28] V. Liu, M. Povinelli, and S. Fan, Resonance-enhanced optical forces between coupled photonic crystal slabs, *Opt. Express* **17**, 21897 (2009).
- [29] E. N. Bulgakov and A. F. Sadreev, Resonant bending of silicon nanowires by incident light, *Opt. Lett.* **45**, 5315 (2020).
- [30] S. Romano, A. Lamberti, M. Masullo, E. Penzo, S. Cabrini, I. Rendina, and V. Mocella, Optical biosensors based on photonic crystals supporting bound states in the continuum, *Materials (Basel, Switzerland)* **11**, 526 (2018).
- [31] K. Ohtaka, Scattering theory of low-energy photon diffraction, *J. Phys. C* **13**, 667 (1980).
- [32] K. Ohtaka, Energy band of photons and low-energy photon diffraction, *Phys. Rev. B* **19**, 5057 (1979).
- [33] K. Ohtaka and M. Inoue, Light scattering from macroscopic spherical bodies. I. Integrated density of states of transverse electromagnetic fields, *Phys. Rev. B* **25**, 677 (1982).
- [34] A. B. Evlyukhin, C. Reinhardt, A. Seidel, B. S. Luk'yanchuk, and B. N. Chichkov, Optical response features of Si-nanoparticle arrays, *Phys. Rev. B* **82**, 045404 (2010).
- [35] Z. Sadrieva, K. Frizyuk, M. Petrov, Y. Kivshar, and A. Bogdanov, Multipolar origin of bound states in the continuum, *Phys. Rev. B* **100**, 115303 (2019).
- [36] J. Jin, X. Yin, L. Ni, M. Soljačić, B. Zhen, and C. Peng, Topologically enabled ultrahigh- q guided resonances robust to out-of-plane scattering, *Nature (London)* **574**, 501 (2019).
- [37] A. Modinos, N. Stefanou, and V. Yannopapas, Applications of the layer-KKR method to photonic crystals, *Opt. Express* **8**, 197 (2001).
- [38] K. Ohtaka, Y. Suda, S. Nagano, T. Ueta, A. Imada, T. Koda, J. S. Bae, K. Mizuno, S. Yano, and Y. Segawa, Photonic band effects in a two-dimensional array of dielectric spheres in the millimeter-wave region, *Phys. Rev. B* **61**, 5267 (2000).
- [39] N. Stefanou, V. Yannopapas, and A. Modinos, Multem 2: A new version of the program for transmission and band-structure calculations of photonic crystals, *Comput. Phys. Commun.* **132**, 189 (2000).
- [40] J. D. Joannopoulos, S. G. Johnson, J. N. Winn, and R. D. Meade, *Photonic Crystals: Molding the Flow of Light*, 2nd ed. (Princeton University Press, Princeton, NJ, 2008).
- [41] *Gratings: Theory and Numeric Applications*, edited by E. Popov (AMU (PUP), Marseille, 2012), Chap. 6, pp. 6.1–6.41.
- [42] J. Jackson, *Classical Electrodynamics* (Wiley, New York, 1999).
- [43] A. Doicu, *Light Scattering by Systems of Particles: Null-Field Method with Discrete Sources: Theory and Programs* (Springer, Berlin, 2006).